Chapter 1

Mean-field dynamo models

We can add to our knowledge, but we cannot subtract from it.

Arthur Koestler
The Sleepwalkers (1959)

Was einmal gedacht wurde,
kann nicht mehr zurückgenommen werden.

Friedrich Dürrenmatt
Die Physiker (1962)

Having established how to circumvent Cowling's theorem by relying on cyclonic small-scale fluid motions, we now construct and investigate the properties of a few simple solar-like axisymmetric mean-field dynamo models in spherical geometry.

1.1 The axisymmetric mean-field dynamo [S5prob]

1.1.1 The dynamo equations

Is was shown in the preceding chapter that the mean-field induction equation for the large-scale component ($\mathbf{B}$) of the magnetic field is

$$\frac{\partial \mathbf{B}}{\partial t} = \nabla \times (\mathbf{u} \times \mathbf{B} + \alpha \mathbf{B} - (\eta_e + \beta) \nabla \times \mathbf{B}) \ , \tag{1.1}$$

The inductive action of the small scale, turbulent flow present in the convective envelope is subsumed into the α- and β-effect term of mean-field theory, as developed in the preceding chapter. It is worth repeating that these are the two terms retained from a (severely) truncated series expansion of the mean electromotive force $\mathcal{E} = \langle \mathbf{u} \times \mathbf{b} \rangle$ associated with the small-scale, fluctuating components of the velocity and magnetic field. You should also recall that the physical conditions under which this truncation can be expected to be meaningful may well not be satisfied under solar interior conditions, and that the rotationally-induced break of axisymmetry which allows to circumvent Cowling's theorem is completely contained in the α-effect. Note finally that, without further ado, we have specialized to the case of scalar α and β, with both, moreover, taken to be functions of the spatial coordinates but not of time.

For the large-scale flow $\mathbf{u}$ we consider again the most general steady 3D axisymmetric flow, including a meridional circulation and large-scale zonal flow:

$$\mathbf{u}(r,\theta) = \mathbf{u}_p(r,\theta) + \varpi\Omega(r,\theta)\hat{\mathbf{e}}_\phi \ , \tag{1.2}$$

where, as before, $\mathbf{u}_p \equiv u_r(r,\theta)\hat{\mathbf{e}}_r + u_\theta(r,\theta)\hat{\mathbf{e}}_\theta$. In what follows we restrict our attention to the *kinematic regime*, corresponding to $\mathbf{u}$ being a specified function of position.

Having thus imposed axisymmetry on the large spatial scales, it is again advantageous to separate the magnetic field into toroidal and poloidal components, the latter expressed as usual in terms of a toroidal vector potential (cf. §**??**). The mean-field induction equation (1.1) is then readily separated into the two components

$$\frac{\partial A}{\partial t} = \eta\left(\nabla^2 - \frac{1}{\varpi^2}\right)A - \frac{1}{\varpi}\mathbf{u}_p\cdot\nabla(\varpi A) + \alpha B \ , \tag{1.3}$$

$$\frac{\partial B}{\partial t} = \eta\left(\nabla^2 - \tfrac{1}{\varpi^2}\right)B - (\nabla\eta)\times(\nabla\times\mathbf{B})$$

$$-\varpi\nabla\cdot\left(\tfrac{B}{\varpi}\mathbf{u}_p\right) + \varpi(\nabla\times A)\cdot(\nabla\Omega) + \nabla\times[\alpha\nabla\times(A\hat{\mathbf{e}}_\phi)] \ , \tag{1.4}$$

which, structurally, only differs from eqs. (**??**)—(**??**) by the presence of two new terms on the RHS associated with the α-effect. Equations (1.3)–(1.4) will hereafter be refered to as the *dynamo equations*. For simplicity of notation, we continue to use η for the net magnetic diffusivity, with the understanding that this now includes the (presumably dominant) contribution

Need to set up $\beta \gg \eta_e$ in MFT chapter

from the β-term of mean-field theory. In general, solutions are sought in a meridional plane of a sphere of radius R, and as with the diffusive problem of §?? are matched to a potential field in the exterior ($r/R > 1$). Regularity requires that the following boundary conditions be imposed on the symmetry axis:

$$A(r,0) = A(r,\pi) = 0, \qquad B(r,0) = B(r,\pi) = 0 \ . \tag{1.5}$$

In practice it is often useful to solve explicitly for mode having odd and even symmetry with respect to the equatorial plane. To do so, one simply solves the dynamo equations in a meridional *quadrant*, and imposes the following boundary conditions along the equatorial plane. For a dipole-like antisymmetric mode,

$$\frac{\partial A(r,\pi/2)}{\partial \theta} = 0, \qquad B(r,\pi/2) = 0 \ , \qquad \text{[Antisymmetric]} \tag{1.6}$$

while for symmetric (quadrupole-like) modes one sets instead

$$A(r,\pi/2) = 0, \qquad \frac{\partial B(r,\pi/2)}{\partial \theta} = 0 \ , \qquad \text{[Symmetric]} \ . \tag{1.7}$$

1.1.2 Scalings and dynamo numbers

Our next step is to put the dynamo equations into nondimensional form. This can actually be carried out in a number of ways. We begin by scaling all lengths in terms of R, and time in terms of the diffusion time $\tau = R^2/\eta$. Equations (1.3)–(1.4) become

$$\frac{\partial A}{\partial t} = \left(\nabla^2 - \frac{1}{\varpi^2}\right) A - \frac{\mathrm{R}_m}{\varpi} \mathbf{u}_p \cdot \nabla(\varpi A) + C_\alpha \alpha B \ , \tag{1.8}$$

$$\frac{\partial B}{\partial t} = \left(\nabla^2 - \tfrac{1}{\varpi^2}\right) B - (\nabla\eta) \times (\nabla \times \mathbf{B}) - \mathrm{R}_m \varpi \nabla \cdot \left(\tfrac{B}{\varpi}\mathbf{u}_p\right)$$

$$+ C_\Omega \varpi (\nabla \times A) \cdot (\nabla\Omega) + C_\alpha \nabla \times [\alpha \nabla \times (A\hat{\mathbf{e}}_\phi)] \ , \tag{1.9}$$

where the following three nondimensional numbers have materialized:

$$C_\alpha = \frac{\alpha_0 R}{\eta_0} \ , \tag{1.10}$$

$$C_\Omega = \frac{\Omega_0 R^2}{\eta_0} \ , \tag{1.11}$$

$$\mathrm{R}_m = \frac{u_0 R}{\eta_0} \ , \tag{1.12}$$

with α_0 (dimension cm s^{-1}), η_0 (dimension cm s^{-1}), u_0 (dimension cm s^{-1} and Ω_0 (dimension s^{-1}) as reference values for the α-effect, diffusivity, meridional flow and shear, respectively. Remember that the functionals α, η, $\mathbf{u}_p$ and Ω are hereafter dimensionless quantities. The quantities C_α and C_Ω are *dynamo numbers*, measuring the importance of inductive versus diffusive effects on the RHS of eqs. (1.8)–(1.9). The third dimensionless number, R_m, is none other than our old friend the magnetic Reynolds number, which measures the relative importance of advection (by meridional circulation) versus diffusion (by Ohmic dissipation) in the transport of A and B in meridional planes.

1.1.3 The $\alpha\Omega$ dynamo equations

In constructing mean-field dynamos for the sun, it has been a common procedure to neglect meridional circulation, on the grounds that it is a very weak flow (but more on this in §1.3 below). In addition, with $R \simeq 7 \times 10^{10}$ cm, $\Omega_0 \sim 10^{-6}$ rad s^{-1}, and $\alpha_0 \sim 100$ cm s^{-1}, one finds $C_\alpha / C_\Omega \sim 10^3$ (independently of the assume dvalue for η_0!), so that on the RHS of eq. (1.9) the shearing term can be expected to dominate over the α-effect term, unless dynamo action is restricted to a very thin layer[1]. On this basis the α-effect term is often omitted in the toroidal component of the induction equation. The resulting, reduced equations define the so-called $\alpha\Omega$ dynamo model:

$$\frac{\partial A}{\partial t} = \left(\nabla^2 - \frac{1}{\varpi^2}\right) A + C_\alpha B \ , \tag{1.13}$$

$$\frac{\partial B}{\partial t} = \left(\nabla^2 - \frac{1}{\varpi^2}\right) B + C_\Omega \varpi (\nabla \times A) \cdot (\nabla \Omega) \ . \tag{1.14}$$

Under this terminology, the original dynamo equations (1.8)–(1.9) describe an $\alpha^2\Omega$ dynamo[2].

[1] What happens then if dynamo action *is* restricted to a very thin spherical shell, for example?

[2] Dynamo action can also occur solely through the α-effect, i.e., without the presence of any large-scale flow. This is called an α^2 dynamo. The dynamos operating in the interior

There is an interesting reciprocal symmetry between eqs. (1.13) and (1.14); the toroidal field production is proportional to the poloidal field strength via the differential rotation. The poloidal field production, in turn, is proportional to the toroidal field strength via the α-effect; schematically,

$$\nabla\Omega \otimes A \rightarrow B \ , \tag{1.15}$$

$$\alpha \otimes B \rightarrow A \ , \tag{1.16}$$

where the symbol "$\otimes$" and "$\rightarrow$" stand for "acting on" and "produces". Evidently we have here —at least conceptually— the ingredients needed for self-regeneration (and exponential growth) of both A and B[3]. Notice that the first of these two steps, the shearing of a large-scale poloidal field by a large-scale differential rotation, has nothing to do with mean-field theory. It will often prove useful to envision dynamo action as the two-step process outlined above; even though both mechanisms operate simultaneously and concurrently, it is quite possible that they in fact do so in spatially distinct regions of the solar interior.

1.1.4 Reformulation as an eigenvalue problem

With α, β and the large-scale flow given, it is certainly possible to integrate the dynamo equations —whether in their $\alpha\Omega$ or $\alpha^2\Omega$ form— as an initial-boundary value problem, subject to some arbitrary initial conditions. Alternately, if none of these functionals depends explicitly on time, one can seek solutions of the form

$$\begin{bmatrix} A(r,\theta,t) \\ B(r,\theta,t) \end{bmatrix} = \begin{bmatrix} a(r,\theta) \\ b(r,\theta) \end{bmatrix} e^{\lambda t} \ , \tag{1.17}$$

where the amplitudes a and b are in general complex quantities. It will prove convenient to write the eigenvalue explicitly as

$$\lambda = \sigma + i\omega \ , \tag{1.18}$$

so that σ is the growth rate and ω the cyclic frequency, both expressed in terms of the inverse diffusion time[4] $\tau^{-1} = \eta/R^2$. Substituting eqs. (1.17) into

---

of the Earth and giant planets are believed to be of this type... at least from the point of view of mean-field theory.

[3]Can you see the similarity here with the mode of operation of the Roberts Cell dynamo, discussed two chapter ago?

[4]In view of our discussion in chapter 3, this then implies that all mean-field dynamo models produced by solution of eq. (1.17) are *by definition* slow dynamos. Can you figure that one out?

the dynamo equations yields a classical linear eigenvalue problem. Because of the non-trivial dependency of the PDE coefficients on spatial coordinates, numerical solutions will be the approach of choice.

In a model for the (oscillatory) solar dynamo, we are looking for solutions where $\sigma > 0$ and $\omega \neq 0$. You may think of a dynamo as a peculiar form of MHD instability! In all models constructed below we used a reference magnetic diffusivity $\eta_0 = 10^{11}\,\mathrm{cm}^2\,\mathrm{s}^{-1}$, so that in dimensional units the dynamo period P is related to the dimensionless frequency ω via

$$P = \frac{9645}{\omega}\ , \qquad [yr]\ . \tag{1.19}$$

Note finally that since the dynamo equations (either in their $\alpha^2\Omega$ or $\alpha\Omega$ form) are linear in A and B, they leave the absolute scale of the magnetic field strength undetermined. We now obtain and study a few simple such solutions.

1.2 A minimal solar-like $\alpha\Omega$ dynamo model [S5solm]

The aim of this section is to construct the simplest but reasonably realistic linear, kinematic $\alpha\Omega$ dynamo model applicable to the Sun. Further refinements will be introduced in subsequent sections. The first thing we need to do is to specify (dimensionless) functional forms for the various flows and other physical quantities appearing in eqs. (1.13)–(1.14). Some of these "ingredients" have been encountered already in earlier chapters, but for later convenience we list them all here again.

1.2.1 Model input: Ω, η, α

For the differential rotation $\Omega(r,\theta)$ we retain our now familiar solar-like parametrization (see also Figure **??**), scaled in terms of the surface equatorial rotation rate:

$$\Omega(r,\theta) = \Omega_C + \frac{\Omega_S(\theta) - \Omega_C}{2}\left[1 + \mathrm{erf}\left(\frac{r - r_C}{w}\right)\right]\ , \tag{1.20}$$

where

$$\Omega_S(\theta) = (1 - a_2\cos^2\theta - a_4\cos^4\theta) \tag{1.21}$$

with parameter values $\Omega_C = 0.939$, $a_2 = 0.1264$, $a_4 = 0.1591$, $r_c/R = 0.713$, and $w/R = 0.05$. In the spirit of producing a model that is solar-like we use a fixed value $C_\Omega = 10^5$, obtained assuming $\Omega_0 = \Omega_{Eq}\Omega_S(0) \sim 10^{-6}$ rad s^{-1} and $\eta_0 \sim 10^{11}$ cm^2 s^{-1}.

For the magnetic diffusivity, we adopt the dimensionless equivalent of the radial profile used in our study of diffusive decay (§**??**, dash-dotted line on Fig. **??**), namely

$$\eta(r) = \Delta\eta + \frac{1-\Delta\eta_c}{2}\left[1+\mathrm{erf}\left(\frac{r-r_c}{w}\right)\right] , \tag{1.22}$$

with the core-to-envelope diffusivity ratio $\Delta\eta \equiv \eta_c/\eta_e$ treated as a model parameter. We restrict ourselves to situations where $\Delta\eta \ll 1$, since we associate η_c with the microscopic magnetic diffusivity, and η_e with the presumably much larger mean-field turbulent diffusivity β [5]. With the microscopic diffusivity $\eta_c \sim 10^4$ cm^2 s^{-1} below the core-envelope interface, and taking the mean-field estimates of β at face value, one obtains $\Delta\eta \sim 10^{-9}$—10^{-6}. The solutions discussed below have $\Delta\eta = 10^{-3}$, which is much larger, but still small enough to nicely illustrate some important consequence of radial gradients in diffusivity.

In the parameter regime characterizing the strongly turbulent solar convection zone, the strength (or even sign) of the α-effect cannot be computed in any reliable manner from first principles, so this will remain the major unknown of the model. In accordance with the $\alpha\Omega$ approximation of the dynamo equations, we restrict ourselves to cases where $|C_\alpha| \ll C_\Omega$. For the dimensionless functional $\alpha(r,\theta)$ we use an expression of the form

$$\alpha(r,\theta) = f(r)g(\theta) , \tag{1.23}$$

where

$$f(r) = \frac{1}{4}\left[1+\mathrm{erf}\left(\frac{r-r_c}{w}\right)\right] \cdot \left[1-\mathrm{erf}\left(\frac{r-0.5(1+r_c)}{w}\right)\right] . \tag{1.24}$$

This combination of error functions concentrates the α-effect in the bottom half of the envelope, and let it vanish smoothly below, just as the net magnetic diffusivity does (i.e., we again set $r_c/R = 0.7$ and $w/R = 0.05$). For reasons that will be discussed presently, we choose $g(\theta)$ so that the α-effect is concentrated at low heliocentric latitudes:

$$g_2(\theta) = \sin^4(\theta)\cos(\theta) . \tag{1.25}$$

[5] We should perhaps repeat that this assumption is a somewhat dubious one, that moreover has been called into question by direct numerical simulation.

The functional $\alpha(r,\theta)$ is everywhere positive in the N-hemisphere and changes sign across the equator ($\theta = \pi/2$), as one would expect from the hemispheric dependence of the Coriolis force. In fact, a simple $\cos(\theta)$ dependency would have been the "minimal" latitudinal dependency compatible with the basic physics of the α-effect in a rotating, stratified, turbulent spherical shell. However, in conjunction with a solar-like differential profile, the use of an α-effect peaking in the polar regions invariably produces a dynamo solution concentrated at high latitude, a consequence of the strong radial shear present there at the core-envelope interface. This is contrary to observational constraints such as the sunspot butterfly diagram. Prevented from tampering much with the differential rotation by helioseismic inversions, one then has no choice but to (artificially!) concentrate the α-effect at low latitudes.

By choosing in this manner an α-effect that "does the right thing", we are throwing away a significant chunk of whatever predictive capability our model might have had. The sad truth is that *ad hoc* specification of the α-effect is a long accepted practice in mean-field dynamo modeling (which of course does not make it any less *ad hoc*!). We proceed nonetheless, keeping mind that the concentration of dynamo activity at low latitudes is henceforth built into our model.

1.2.2 The $\alpha\Omega$ eigenvalues

Ref to numerical appendix

Armed (and dangerous) with the above model, we plow ahead and solve the $\alpha\Omega$ as en eigenvalue problem, using inverse iteration (see appendix XX) We first produce a sequence of solutions for increasing values of $|C_\alpha|$, holding C_Ω fixed at a "solar" value 10^5, and without meridional circulation ($\mathrm{R}_m = 0$)[6]. Figure 1.2.2 shows the variation of the growth rate σ and frequency ω as a function of C_α. Four sequences are shown, corresponding to modes that are either antisymmetric or symmetric with respect to the equatorial plane ("A" and "S" respectively), computed with either positive or negative C_α. For $|C_\alpha|$ smaller than some threshold value, the induction terms make too small a contribution to the RHS of eq. (1.13), leaving the dissipation terms dominant, so that solutions all have $\sigma < 0$, as per Cowling's theorem. As $|C_\alpha|$ increases, the growth rate eventually reaches $\sigma = 0$. At this point we also have $\omega \neq 0$, so that the corresponding solution oscillates with neither

[6] Obtaining such sequences by inverse iteration is easy if one uses the eigenvalue obtained for a given value of C_α as a guess for the eigenvalue of the next solution incremented in C_α. The first eigenvalue of the sequence must be hunted down by trial and error, or estimated using a different numerical technique (see Appendix XX).

growth of decay of its amplitude. Further increases of $|C_\alpha|$ lead to $\sigma > 0$. We are now finally in the dynamo regime, where a weak initial field is amplified exponentially in time.

Computing similar sequences for the same same model but different values of C_Ω soon reveals than the onset of dynamo activity ($\sigma > 0$) is controlled by the *product* of C_α and C_Ω:

$$D \equiv C_\alpha \times C_\Omega = \frac{\alpha_0 \Omega_0 R^3}{\eta_0^2}. \tag{1.26}$$

The value of D for which $\sigma = 0$ is called the *critical dynamo number* (denoted $D_{\rm crit}$)[7]. This, at least, is similar to what we found for the analytical solution of §4.XX[8] Modes having $\sigma < 0$ are called *subcritical*, and those having $\sigma > 0$ *supercritical*. Note on Fig. 1.2.2 how relatively little the growth rate and dynamo frequency depend on the assumed solution parity. For the model of Figure 1.2.2, the first mode to become supercritical is the negative C_α antisymmetric mode, for which $D_{\rm crit} = -1.60 \times 10^5$, followed shortly by the negative C_α symmetric mode ($D_{\rm crit} = -1.76 \times 10^5$). The dynamo frequency for these critical modes is $\omega \simeq 250$, which corresponds to a full cycle period of $\sim 40\,$yr for a reference magnetic diffusivity $\eta_0 = 10^{11}\,{\rm cm}^2\,{\rm s}^{-1}$. This is within a factor of two of the observed full solar cycle period. Once again we should not be too impressed by this, since we have quite a bit of margin of manoeuver in specifying numerical values for η_0 and C_α, and there is no reason to believe that the Sun should be exactly exactly at the criticasl threshold for dynamo action. Moreover, it is readily verified that above criticality, the eigenvalue scales as

Ref to mean-field chapter

$$\sigma, \omega \propto \sqrt{D}\ , \qquad , D \gtrsim D_{\rm crit}\ , \tag{1.27}$$

so that an increase of $|C_\alpha|$ to a value $-1.XX$, readily yields a (supercritical) solution with period $\sim 22\,$yr.

1.2.3 The $\alpha\Omega$ eigenfunctions

Back in §**??**.3 we showed that the shearing of a poloidal field by our solar-like differential rotation profile produced a toroidal field strongly concentrated

[7] Can you find a way of scaling the $\alpha\Omega$ dynamo equations so that the only nondimensional number appearing in the scaled version of the equation is the dynamo number D defined above?

[8] ...but does not hold for $\alpha^2\Omega$ dynamo solutions!

in the vicinity of the core-envelope, in view of the strong radial shear present there (see Figs. **??** and **??**). Not surprisingly, this property carries over to the $\alpha\Omega$ eigenfunctions.

Figure 1.2.3 shows a close up of the toroidal eigenfunction in the shear layer, at four successive equally-spaced phase intervals covering half an oscillation cycle. With $\sigma = 15.8$ and $\omega = 307$, this $C_\alpha = 2$ solution is supercritical although in generating Figure 1.2.3 (and Fig. 1.2.3 further below) the growth rate σ was artificially forced to zero, so that the solution snapshots at $\varphi = 0$ and π are strictly identical... except for a *magnetic polarity reversal* in both the toroidal and poloidal components.

Need to update values here

Examination of 1.2.3 soon reveals that the toroidal flux systems of opposite magnetic polarity present in the equatorial part of the shear layer first show up at mid-latitutes, and then *migrate equatorward* to finally disappear near the equatorial plane in the course of the half-cycle[9]. This migration is poleward in the positive C_α solutions. If you haven't already guessed it, what we are seeing on Figure 1.2.3 is the spherical equivalent of the dynamo waves investigated in §**??** for the cartesian case with uniform α-effect and shear. If we identify r with z and θ with x, we have indeed the correct sense of propagation for a positive radial shear and negative α-effect.

Check with TJB on his coordinate definitions

Careful scrutiny of the toroidal field contours on Figure 1.2.3 also reveals that the toroidal field peaks somewhat *below* the depth we identified with the core-envelope interface (dashed line), where, in view of eqs. (1.20)—(**??**), the radial shear is maximal and the magnetic diffusivity and α-effect are undergoing their fastest variation with depth. This is the diamagnetic effect in action (cf. §**??**.4), i.e., spatial concentration of the magnetic field in regions of lower η. But why is the amplitude of the eigenfunctions vanishing so rapidly below the core-envelope interface? After all, the poloidal and toroidal diffusive eigenmodes investigated in §**??** were truly global, and the diamagnetic effect should favor stronger fields in the lower diffusivity core. The crucial difference lies with the oscillatory nature of the solution: because the magnetic field produced in the vicinity of the core-envelope interface is oscillating with alternating polarity, its penetration depth in the core is limited by the electromagnetic skin depth $\ell = \sqrt{2\eta_c/\omega}$ (§**??**), with η_c the core diffusivity. Having assumed $\eta_0 \equiv \eta_e = 10^{11}\,\mathrm{cm^2\,s^{-1}}$, we have $\eta_c = \eta_e \Delta\eta = 10^8\,\mathrm{cm^2\,s^{-1}}$. A dimensionless dynamo frequency $\omega \simeq 300$ corresponds to $\simeq 10^{-9}\,\mathrm{s^{-1}}$, so that $\ell/R \simeq 0.006$, quite small indeed.

[9]An animation of this solution, as well as the one discussed next, can be viewed on the course Web Page.

Another useful way to look at our solutions is to construct a diagram where the poloidal or toroidal field evaluated on a sphere of constant radius are plotted against polar angle and phase of the cycle. Such a diagram is shown on Figure 1.2.3, again for the $C_\alpha = -2$ solution of Figs. 1.2.3. The horizontal axis (phase φ) is equivalent to time, and the equator is at $\cos(\theta) = 0$. The equatorward migration of both toroidal and poloidal fields —here its radial component B_r— is clearly apparent on this diagram, together with the fact that the solution is antisymmetric about the equator. The propagation of dynamo waves shows up as a "tilt" of the flux contours away from the horizontal direction.

The toroidal field cut (part [A]) is computed at $r/R = 0.7$, i.e., the location in our model one would associate with the base of the convective envelope. Now, *if* this is indeed where the toroidal flux ropes that become sunspots originate, *if* they rise radially throughout the convective envelope, and *if* their rise time is short compared to the duration of the cycle, then Fig. 1.2.3(A) can be compared to the sunspot butterfly diagram. The two diagrams actually compare quite well; The toroidal field of a new cycle first appears at mid-latitudes, and reaches its maximal strength in the course of its equatorward migration. There is perhaps a little too much temporal overlap between the flux systems of two successive cycles. Note also that the surface poloidal field is much weaker than the toroidal field in the shear layer (you get to further explore the origin of this model behavior in problem 5.X), in agreement with observational inferences, but its surface evolution shows little resemblance to observations.

Appropriate Ref. to part III here

Need sunspot butterfly diagram and surface magnetogram

1.3 Enter Meridional circulation [S5.cm]

As a further step to bring our minimal mean-field solar dynamo model hopefully closer to reality, we now reintroduce a meridional flow $\mathbf{u}(r, \theta)$ in the $\alpha\Omega$ dynamo equations (1.13)–(1.14). We otherwise retain the same model and parameter values as in the preceding section.

In spherical polar coordinates an axisymmetric meridional flow can expressed in terms of a stream function $\Psi(r, \theta)$ as

$$\mathbf{u}_p(r, \theta) = \frac{u_0}{\rho r \sin\theta} \left[\frac{1}{r} \frac{\partial \Psi}{\partial \theta} \hat{\mathbf{e}}_r - \frac{\partial \Psi}{\partial r} \hat{\mathbf{e}}_\theta \right] . \quad (1.28)$$

Note the appearance of the long-lost density (ρ), whose presence is required to ensure that $\nabla \cdot (\rho \mathbf{u}) = 0$. We choose a stream function of the form

$$\Psi(r,\theta) = 2\left[\frac{(r-r_0)^3}{(R-r_0)^2} - \frac{(r-r_0)^2}{(R-r_0)}\right]\sin^2\theta\cos\theta, \qquad r \geq r_0 \tag{1.29}$$

and $\Psi = 0$ otherwise. This defines a quadrupolar flow (i.e., one flow cell per meridional quadrant) contained between the spherical shells $r = r_0$ and $r = R$. For $u_0 > 0$ the flow is poleward at the surface, with speed $u_\theta(R, \pi/4) = u_0$, and vanishes smoothly as $r \to r_0$, i.e., $\mathbf{u}(r_0,\theta) = u_\theta(r_0,\theta)\hat{\mathbf{e}}_\theta \to 0$. Current helioseismic determinations of the circulation speed in the upper third of the envelope indicate $u_0 \simeq 1500\,\mathrm{cm\,s^{-1}}$, which translates to $\mathrm{R}_m \simeq 10^3$ for $\eta = 10^{11}\,\mathrm{cm^2\,s^{-1}}$. The meridional flow streamlines are plotted on Figure 1.3, together with a profile of the latitudinal flow speed u_θ along a radial cut at mid-latitudes ($\theta = \pi/4$). A value $r_0/R = 0.65$ is used, which implies that the flow penetrates slightly below the nominal core-envelope interface at $r_c/R = 0.7$, in agreement with some recent numerical simulations results (see bibliography).

For the specification of the density profile, it is sufficient to approximate the convection zone by a polytropic shell of index $\alpha = 5/3$, ignoring self-gravity in the shell and using physical conditions at the base of the envelope to set the scale height (see dash-dotted line on Figure 1.3B)[10]. The density varies by three orders of magnitude from the base of the envelope to the surface, so that the return flow at mid latitude $u_\theta(r_c, \pi/4) \simeq -5 \times 10^{-4}\,u_0$. The effect of the meridional flow can thus be expected to be less pronounced deep in the envelope than near the surface.

Ref to part I here

Our first task is to investigate the effect of meridional circulation on the parity, growth rate, and dynamo period of the model. This is carried out on Figure 1.3, showing the variation of the growth rate and frequency for two sequences of solutions with increasing R_m. The dynamo numbers are $C_\alpha = -4$ and $C_\Omega = 10^5$, so that the solutions are directly comparable to that discussed earlier in §1.2. Curves are shown for the antisymmetric and symmetric fastest growing modes; recall that in the absence of meridional circulation the symmetric (quadrupole-like) mode is fastest growing at these values of the dynamo number (though very slightly so, $\sigma(A) = 5.43$ vs $\sigma(S) = YYY$; see also Fig. 1.2.2).

[10]Having prescribed the stream function in a pretty arbitary manner, a very accurate representation of the density profile would not add much realism to our meridional circulation model; its physical relevance —or lack thereof— rests primarily on the choice of stream function.

Let us return to the $\mathrm{R}_m = 10^3$ solution, which has a solar-like surface meridional flow speed. Butterfly diagrams for this solution are shown on Figure 1.3, in the usual format. This should be compared to Fig. 1.2.3, which is a $\mathrm{R}_m = 0$ but othewise identical solution. Evidently the toroidal field distribution at the base of the envelope has hardly changed. This can be understood upon noting that even though $\mathrm{R}_m \gg 1$ at the surface, the marked decrease with depth of the circulation speed that results from the rapidly increasing density means that the *effective* local Reynolds number at the base of the envelope is actually ~ 0.5, which indicates that advection by the circulation is weaker than diffusive transport. One notable difference with Fig. 1.2.3 is the appearance of a small, weak polar branch at high latitudes. This is again a manifestation of dynamo action occurring via the negative radial shear in the high latitude portion of the shear layer (notice the poleward propagation), although for this value of R_m the equatorward branch still dominates.

Meridional circulation has a greater effect on the surface fields, however, as becomes apparent upon comparing Figs. 1.2.3B and 1.3B. Note in particular on Fig. 1.3B the presence of a well-defined polar branch, corresponding to the poleward advection by the meridional circulation of the poloidal field that emerges at low latitudes (and pretty much remains there in the absence of circulation, see Figs. **??** and 1.2.3B). Better yet, the reversal of the polar field branch occurs very near the time of "sunspot maximum", i.e., peak toroidal field at the base of the envelope (Fig. 1.3A). This is precisely the phase relationship observed on the Sun!

The inclusion of meridional circulation ha thus improved our minimal $\alpha\Omega$ model at two levels: it has produced a surface radial field distribution/evolution in better agreement with observations, and has restored the dominance of the A modes as the fastest growing, at least in the linear regime. This is about as far as we can should with linear models. We now examine whether some or all of these favorable features persist in the nonlinear regime.

1.4 Nonlinear $\alpha\Omega$ dynamos

1.4.1 The inexorably growing Lorentz force

1.4.2 α-quenching and other dirty shortcuts

1.4.3 An α-quenched dynamo solution

1.5 Stochastic fluctuations

1.5.1 The α-effect as a statistical average

1.5.2 A stochastically fluctuating, α-quenched dynamo solution

---

Problems:

The following problems may seem a bit overwhelming at first sight, but stick to it and they all work out much more easily than you might expect. The objective is to get you to play with a numerical dynamo code, in fact the very same code used to generate the solutions discussed in §§5.2 and 5.3, in order to investigate certain general properties of kinematic linear mean-field dynamo models[11]. If you don't have a computer account on a system where IDL is available, get in touch with one of us and we'll organize to give you access to a suitable guest account on the HAO computer systems.

For any of the following problems, once again your first step is to go to the course Web Page:

`http://www.hao.ucar.edu/public/education/astr7500.html`

Click on *Problems: Software and hints*, find the appropriate subsection, and from there grab the following four files[12]:

1. `sphdyn_eig.f`
2. `medplane.idl`
3. `butterfly.idl`

[11] As further incentive to give it a try let us hint that there is an *extremely* high probability that one of these problems will end up on the final exam...

[12] If you are completely Web-Phobic or do not have a Web Browser at your disposal, the files can be sent to you via e-mail. Just send e-mail to `paulchar@hao.ucar.edu` requesting it.

4. `README.txt`

The file `sphdyn_eig.f` is a fully self-contained standard Fortran-77 source code, profusely commented, that computes a dynamo eigenvalue and eigenvector using inverse iteration. The user must supply two fortran functions (examples are included in the file) that calculate the α-effect and angular velocity Ω as a function of r and θ. The user must also supply numerical values for the two dynamo numbers C_α and C_Ω, as well as a trial eigenvalue to begin the inverse iteration.

Upon successful completion, the fortran code produces a single output file (`solution.i3e`; IEEE unformatted). The two files `medplane.idl` and `butterfly.idl` are IDL source codes that are set up to read in this output file, and produce plots of the solution in meridional planes, and a butterfly diagram, basically as on Figures 1.2.3 and 1.2.3 above. Both IDL codes also include numerous informative comments. The file `README.txt` is a plain ASCII text file that contains some general information on how to compile fortran code under Unix operating systems, how to run programs in IDL, create printable postscript files, etc.

Once you have the files set up on your computer account, your first step will be to verify that all is working properly and make sure that you have under control the various steps required to produce a solution. Toward that end, you should recompute the dynamo solution of Figs. 1.2.3 and 1.2.3. Once you are satisfied with this first test, then you are ready use your newly acquired dynamo modeling skills for working out the following problems:

1. Using the angular velocity and α-effect profiles given by eqs. (5.10) and (5.11), investigate the behavior of the average B_r/B_ϕ for near-critical dynamo modes obtained for various values and sign combinations of C_α and C_Ω, but for constant D (cf. eq. [5.13]).

2. For the α-effect profile given by eq. (5.11), construct a series of near-critical dynamo solutions for 4 distinct differential rotation profiles: purely radial differential rotation, with $\partial\Omega/\partial r > 0$ and < 0, and purely latitudinal differential rotation, with $\partial\Omega/\partial\theta > 0$ and < 0. Study your solutions and try to establish a general rule for the propagation of dynamo waves.

3. The aim with this one is to have you establish scaling laws (if any exist) relating the growth rate σ and dynamo frequency ω to the magnitudes of C_α and/or C_Ω. To address this question you need to obtains series of

eigenvalues for different dynamo numbers, for which you may want to proceed as follows: sticking again to the α-effect and angular velocity profiles defined by eqs. (5.11) and (5.14) and with negative C_α, and starting from a near-critical solution, construct three sequences of 10 solutions covering two orders of magnitude in dynamo numbers, for

(a) $C_\Omega = |C_\alpha|$ (equivalent to Fig. 5.1), both increasing;

(b) C_Ω fixed, $|C_\alpha|$ increasing;

(c) C_α fixed, C_Ω increasing.

4. Construct a solution for a magnetic diffusivity that varies with depth, but otherwise identical to the negative C_α solution of §5.2. This will involve modifying the function `dmagxy` in the file `sphdyn_eig.f`. Examine the effect of lowering the magnetic diffusivity η in the core portion of the domain; toward this end you may use something like the radial dependency of η used in §5.3, but with with $0.001 \leq \eta_c \leq 1$, $r_c = 0.7$ and $w = 0.2$. Discuss similarities and differences with the constant-η solution of §5.2.

5. Construct two solution sequences of increasing dynamo numbers (as in Fig. 5.1) for $C_\Omega = |C_\alpha|$ with C_α either positive or negative, for *quadrupolar* dynamo modes. In its basic form, the code `sphdyn_eig.f` solves over a full meridional quadrant and so does not pose any constraint as to the parity of the modes on which the algorithm converges. It is however possible to enforce the preferential selection of either dipolar or quadrupolar modes by setting the control parameter `ipar` to integer values different from zero (details given in the code itself). You can use any of the $\Omega(r, \theta)$ profiles used in this chapter.

   (a) Compare the eigenvalue distributions of your quadrupolar sequences to those of otherwise similar dipolar sequences. Which mode is most easily excited ? Can you think of a reason why ?

   (b) Plot your two nearest-critical solutions for positive and negative C_α. How does their dynamo wave propagation direction compare with that of the dipolar modes ?

Bibliography:

Mean field models for solar and planetary dynamos were first discussed by

Steenbeck, Krause, F. 1969, Astr. Nach., 291, 49,

But the manifesto of the Potsdam school of dynamo modeling is the book

Krause, F., & Rädler, K.-H. 1980, *Mean-field electrodynamics and dynamo theory*, (Oxford: Pergamon Press).

Mean-field solar dynamo modeling can be divided in two epochs: pre- and post-helioseismology. In the former, the solar internal differential rotation is a free function. In the latter it no longer is. Linear solutions in spherical geometry similar to those described in §5.2 belong to the first epoch, and are discussed in detail in

Stix, M. 1976, *Astron. Ap.*, **47**, 243,

with particular attention to critical modes, parity, and phase relationship between the poloidal and toroidal components. Other noteworthy papers from this epoch are:

Deinzer, W., & Stix, M. 1971, *Astron. Ap.*, **12**, 111,
Lerche, I., & Parker, E.N. 1972, *Astrophys. J.*, **176**, 213,
Yoshimura, Y. 1975, *Astrophys. J.*, **201**, 740,
Ivanova, T.S., & Ruzmaikin, A.A. 1976, Sov. Astron., 20, 227.

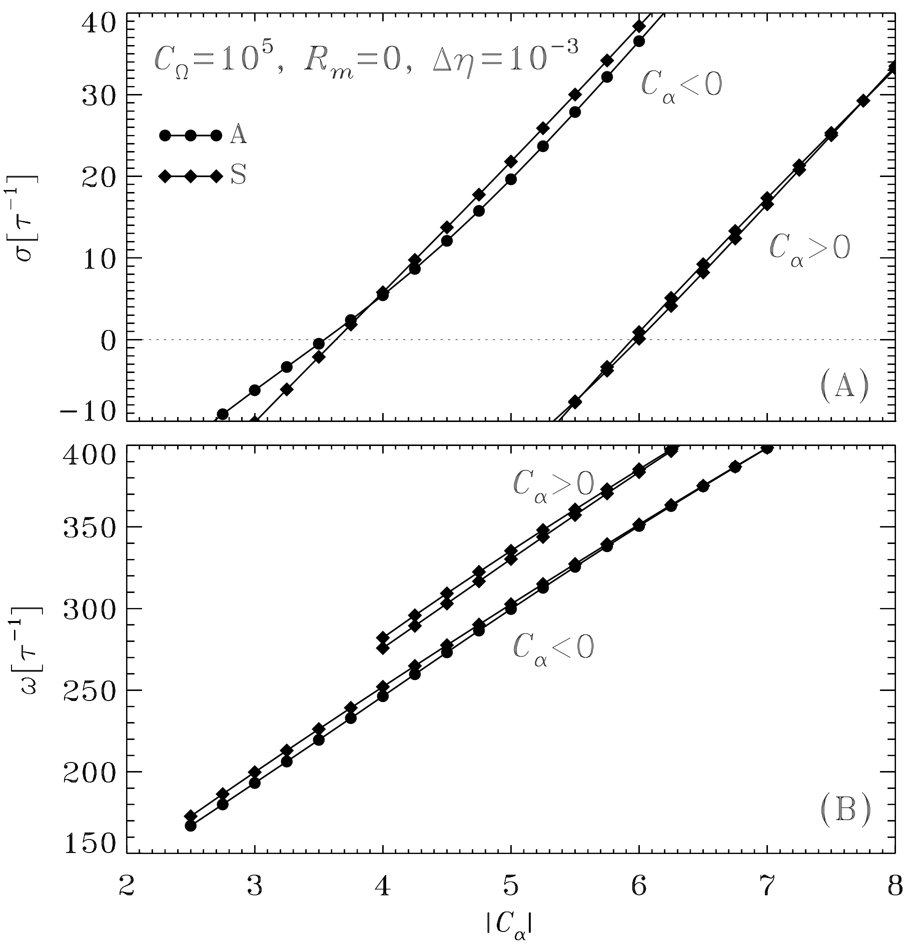

Figure 1.1: [F5.1] Variations of the dynamo growth rate (A) and frequency (B) as a function of increasing $|C_\alpha$— in the minimal $\alpha\Omega$ model. Sequences are shown for either positive or negative dynamo number (as labeled), and symmetric (diamonds) or antisymmetric (dots) parity. Modes having $\sigma < 0$ are decaying, and modes with $\sigma > 0$ exponentially growing. Note how modes with A or S parity have nearly identical eigenvalues. In this model the first mode to reach criticality is the negative C_α A mode, for which $D_{\mathrm{crit}} = -1.60 \times 10^5$.

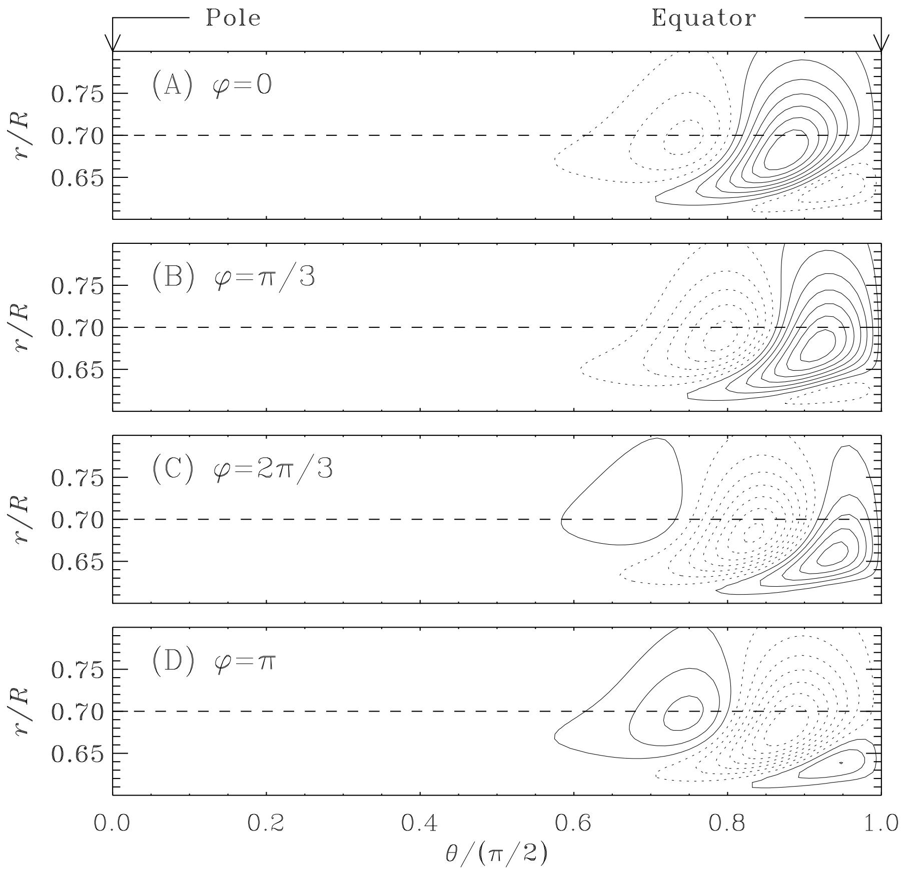

Figure 1.2: [F5.3] Cartesian close up of the toroidal eigenfunction in the vicinity of the core-envelope interface ($r/R = 0.7$, dashed line on each panel). The real part of the toroidal eigenfunction is plotted as isocontours, at four successive and equally spaced phase intervals covering half an oscillation cycle. Solid (dotted) contours correspond to positive (negative) $b(r, \theta)$. Note the equatorward propagation of the toroidal flux systems, and how the toroidal field actually peaks slightly below the core-envelope interface.

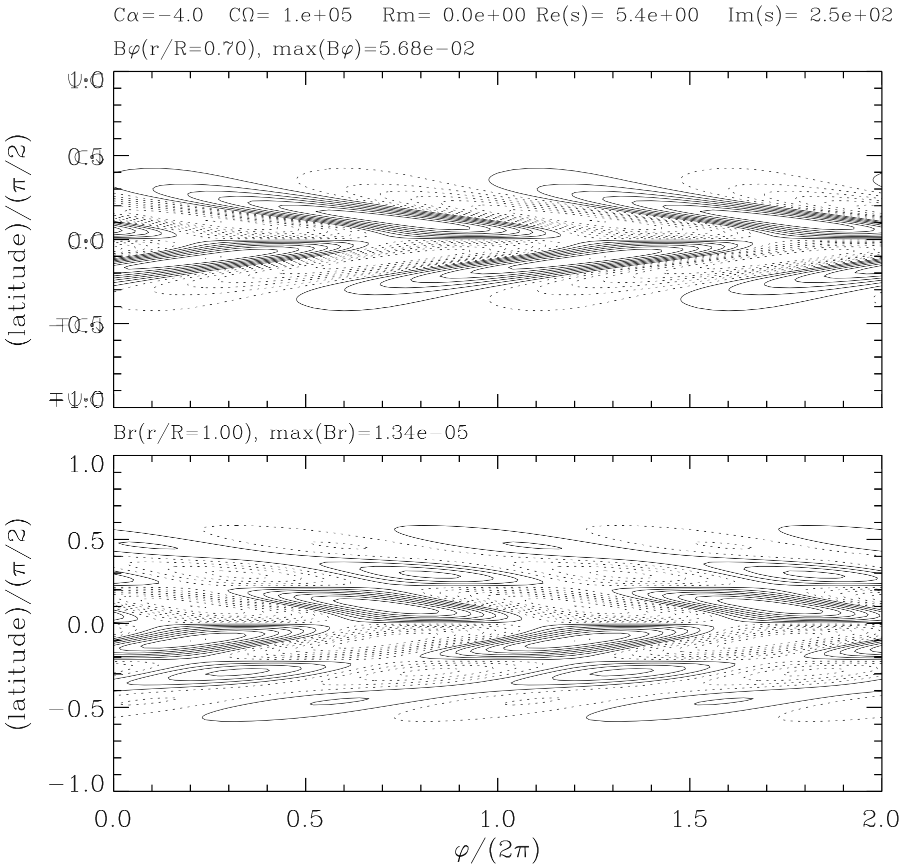

Figure 1.3: [F5.4] Butterfly diagram for the $C_\alpha = -4$ $\alpha\Omega$ solution of Figures 1.2.3. Butterfly diagram are constant depth, 2-D plots of a dynamo solution in latitude-time/phase space. The top panel shows contours of toroidal field B_ϕ at $r/R = 0.7$. Solid (dotted) contours correspond to positive (negative) toroidal field, with contour spacing $\Delta B_\phi = 0.1333$. The field has been normalized to its maximum value in the course of the cycle. The bottom panel shows the radial component of the poloidal field at the surface ($r/R = 1$).

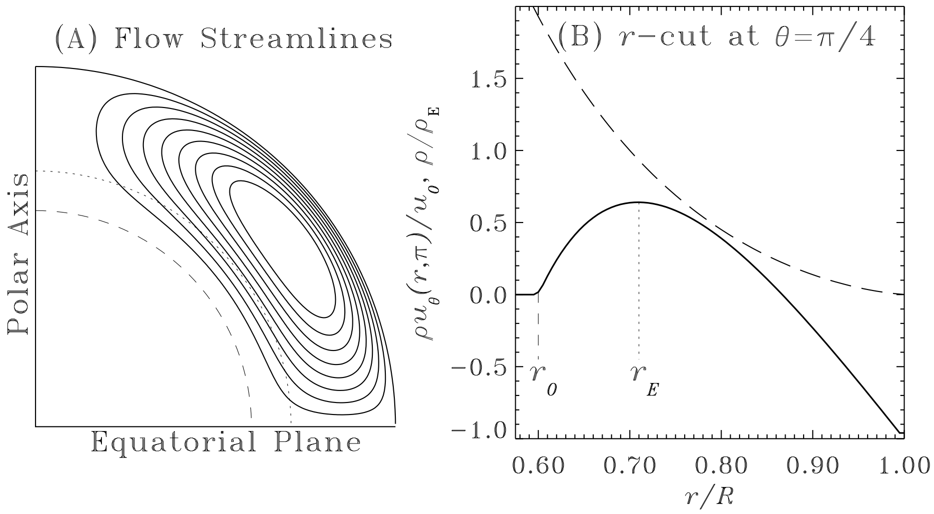

Figure 1.4: [F5.9] A solar-like meridional flow profile, constructed using the stream function given by eq. (1.29), with $r_0/R = 0.6$. Part A shows the flow streamlines in a meridional quadrant, and part B a profile of the latitudinal flow speed u_θ along a radial cut at $\theta = \pi/4$. The dash-dotted line is a polytropic density profile (see eq. I.X.Y) with index 5/3 and base temperature $2 \times 10^6\,K$, normalized to the density at the core-envelope interface.

Antisymmetric

Symmetric

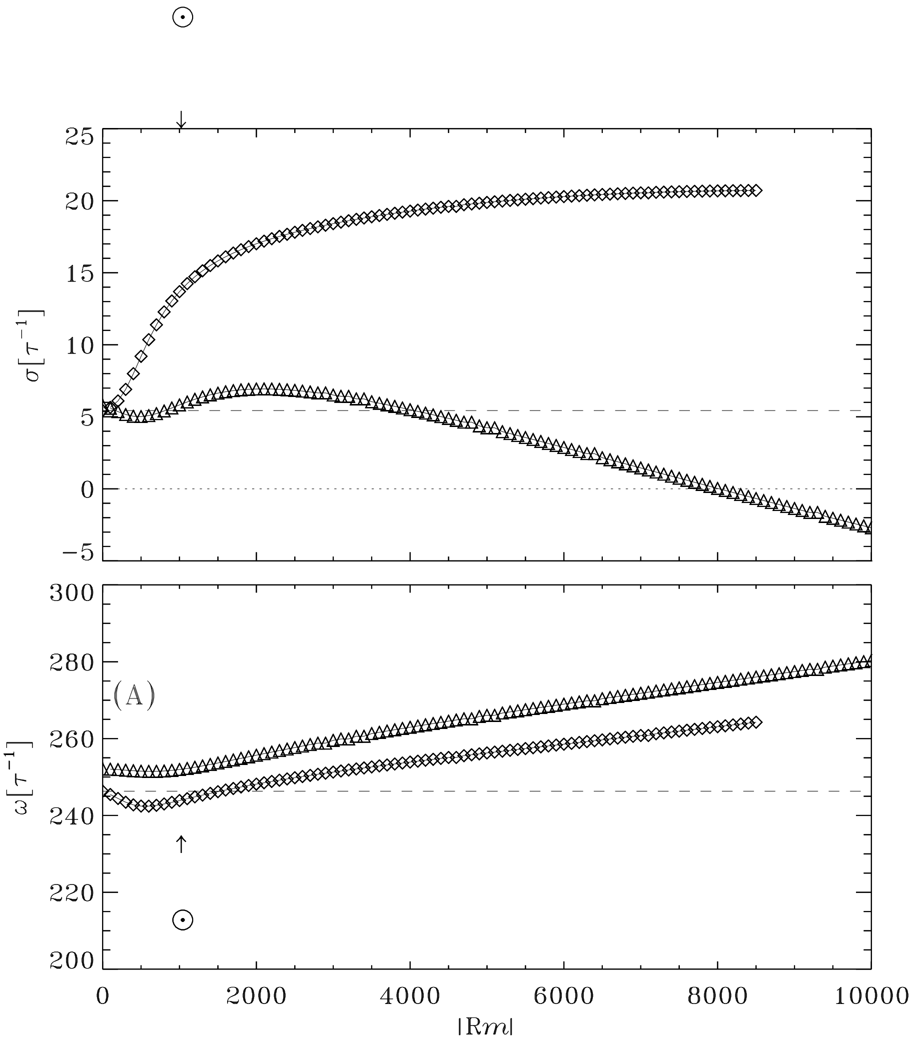

Figure 1.5: [F5.10] Variation of the dynamo growth rate (A) and frequency (B) for a sequence of solution with solar-like meridional circulation and differential rotation, for increasing meridional flow speed u_0 as measured by the Reynolds number R_m (see eq. (1.12)). For the Sun, $u_0 \simeq 1500\,\mathrm{cm\,s^{-1}}$ corresponds to $\mathrm{R}_m = 10^3$, for $\eta = 10^{11}\,\mathrm{cm^2\,s^{-1}}$. All solutions have $C_\alpha = -4$, $C_\Omega = 10^5$, and $\Delta\eta = 10^{-3}$. Diamonds (triangles) identify antisymmetric (symmetric) solutions. rates (see text).

$C\alpha = -4.0,\ C\Omega = 10^5$

(B)

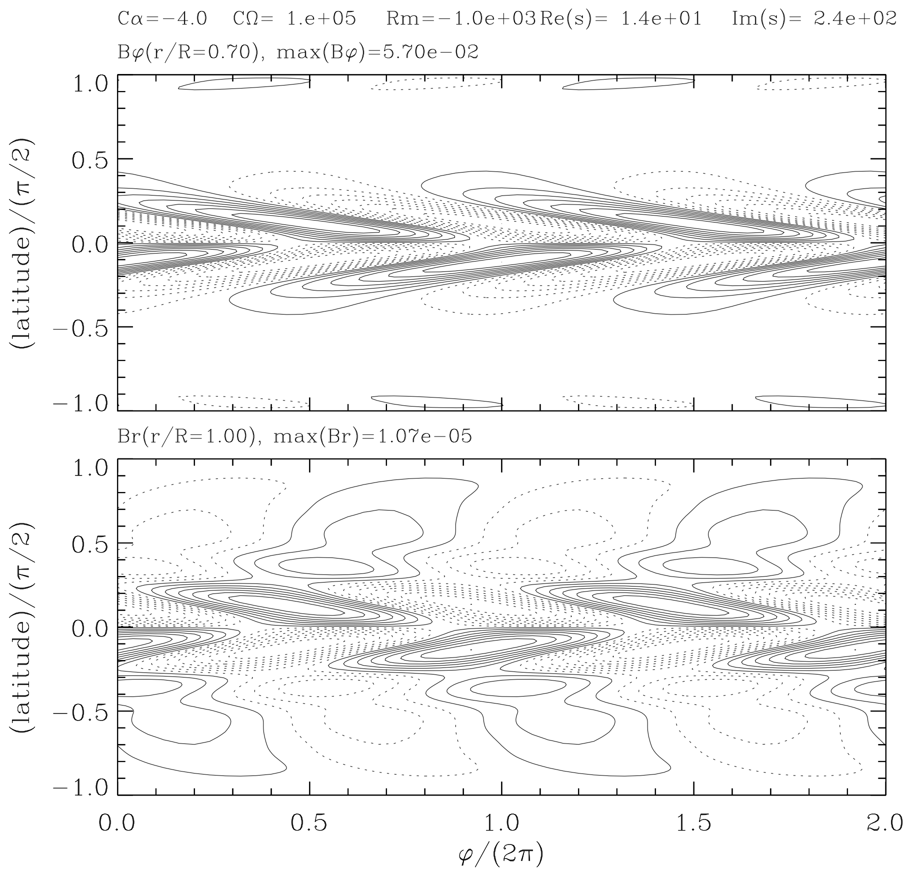

Figure 1.6: [F5.11] Butterfly diagram for a solution with solar-like meridional circulation and differential rotation. Solution parameters are $C_\alpha = -4$, $C_\Omega = 10^5$, $\Delta\eta = 10^{-3}$, and $\mathrm{R}_m = 10^3$. This Figure should be compared to Figure 1.2.3, to appreciate the effect of circulation on the surface poloidal field (bottom panels). Note how the polar surface field on part B reverses polarity at about the time at which the toroidal field peaks at the base of the envelope (part A). This is in agreement with observations.